AIP | Physics of Fluids

Nonlinear interaction of two waves in boundarylayer flows

Ali H. Nayfeh and Ali N. Bozatli

Citation: Physics of Fluids (1958-1988) **23**, 448 (1980); doi: 10.1063/1.863013
View online: http://dx.doi.org/10.1063/1.863013
View Table of Contents: http://scitation.aip.org/content/aip/journal/pof1/23/3?ver=pdfcov
Published by the AIP Publishing

Nonlinear interaction of two waves in boundary-layer flows

Ali H. Nayfeh and Ali N. Bozatli[a)]

Department of Engineering Science and Mechanics, Virginia Polytechnic Institute and State University, Blacksburgh, Virginia 24061
(Received 5 February 1979; accepted 30 November 1979)

First-order nonlinear interactions of Tollmien–Schlichting waves of different frequencies and initial amplitudes in boundary-layer flows are analyzed using the method of multiple scales. Numerical results for flow past a flat plate show that the spatial detuning wipes out resonant interactions unless the initial amplitudes are very large. Thus, a wave having a moderate amplitude has little influence on its subharmonic although it has a strong influence on its second harmonic. Moreover, two waves having moderate amplitudes have a strong influence on their difference frequency. The results show that the difference frequency can be very unstable when generated by the nonlinear interaction, even though it may be stable when introduced by itself in the boundary layer.

I. INTRODUCTION

One of the major roads from laminar to turbulent flow involves the initial linear amplification of disturbances which might be present in the flow. However, as these disturbances grow to appreciable amplitudes, nonlinear effects set in. The nonlinear mechanisms that are activated depend on the spectrum of the disturbances. In this paper, we investigate two of these mechanisms.

In his experiments on the transition from laminar to turbulent flow in a separated shear layer, Sato[1] observed the appearance of the subharmonic of order one-half in addition to the higher harmonics of the fundamental wave. Wille[2] observed the development of subharmonic waves while investigating the stability of both circular and plane jets. Kachanov *et al.*[3] observed that, in addition to the higher harmonics of a fundamental wave, which was introduced in the flow by a vibrating ribbon, a subharmonic wave with one-half the frequency of the fundamental wave appeared downstream. Kelly[4] showed that the appearance of the subharmonic in a shear layer is due to a secondary linear instability associated with a time-dependent flow that consists of the superposition of the basic flow and a finite-amplitude fundamental wave. Nayfeh and Bozatli[5] investigated the appearance of the subharmonic in boundary layers by analyzing the instability associated with a time-dependent flow that consists of the superposition of the basic flow and a Tollmien–Schlichting wave. The results show that the amplitude of the fundamental wave must exceed a critical value to trigger this parametric instability. This value is proportional to a detuning parameter that is the real part of $k-2K$, where k and K are the wavenumbers of the fundamental and its subharmonic, respectively. For the Blasius flow, the critical amplitude is approximately 29% of the mean flow. For other flows where the detuning parameter is small, such as free-shear layer flows, the critical amplitude can be small; thus, the parametric instability might play a greater role. Since the analysis of Kelly[4] and Nayfeh and Bozatli[5] are linear, they do not account for the effect of the subharmonic wave on the fundamental wave. This effect may be small initially, but as the subharmonic grows appreciably, its effect on the fundamental cannot be neglected. One of the purposes of the present paper is to determine the nonlinear interaction of a Tollmien–Schlichting wave with its subharmonic.

Sato,[6] Miksad,[7] Kachanov *et al.*,[8] and Saric and Reynolds[9] observed that the nonlinear development of the waves in the transition region depends on the initial and external disturbances. Sato[6] conducted an experiment on the stability of symmetric laminar waves by exciting two unstable modes with the frequencies f_1 and f_2. He observed the generation of waves having the frequencies $f_2 \pm f_1$. Miksad[7] excited two unstable modes of a laminar asymmetric free-shear layer. He also observed nonlinear triggered instabilities of the difference mode $f_2 - f_1$, subharmonics, and higher harmonics of the fundamental waves. Kachanov *et al.*[8] introduced two Tollmien–Schlichting waves in the boundary layer on a flat plate by using two vibrating ribbons. They observed the appearance and growth of a Tollmien–Schlichting wave having the difference frequency $f_2 - f_1$. Norman[10] also observed the amplification of the difference harmonic of two introduced disturbance waves in his experimental study of secondary flows around and downstream of protuberances in laminar boundary layers. The second purpose of the present paper is to determine the nonlinear interaction of three Tollmien–Schlichting waves (combination resonance) in boundary layers and to show that the difference frequency can be very unstable when generated by the nonlinearity, even though it is stable when introduced by itself in the boundary layer.

The possibility of resonant wave interactions in boundary-layer flows has been recognized by Craik[11] and the consequences of such interactions have been investigated in a number of papers by Craik and co-workers, see for example Refs. 12 and 13 for their latest results. Craik and co-workers considered the interaction of three waves with the wavenumbers $\mathbf{k}_1$, $\mathbf{k}_2$, and $\mathbf{k}_3$ corresponding to the frequencies ω_1, ω_2, and ω_3 and satisfying the conditions

[a)] Present address: Engineering Science Department, University of Arkansas, Fayetteville, Ark. 72701.

 0031-9171/80/030448-11$00.90

$$\mathbf{k}_1 \pm \mathbf{k}_2 \pm \mathbf{k}_3 = 0, \quad \omega_1 \pm \omega_2 \pm \omega_3 = 0 .$$

Under these conditions, they found an explosive instability. However this explosive instability occurs only when the above resonances are perfectly satisfied. In a boundary layer, however, the resonances are perfectly tuned only at a single location due to spatial detuning. The present results for two-dimensional waves and those in Ref. 14 for three-dimensional waves show that the explosive instability does not occur in a boundary layer. Moreover, the present results, as well as those in Ref. 5, indicate that a two-dimensional wave in a boundary layer on a flat plate cannot affect its two-dimensional subharmonic unless its amplitude exceeds about 29% of the mean flow, when the boundary layer has already become turbulent. In the case of a boundary layer on a flat plate, Nayfeh and Bozatli[14] found that a two-dimensional wave does not appreciably affect its subharmonic oblique waves due to spatial detuning unless the two-dimensional wave is unstable. They proposed a four-wave interaction in which a two-dimensional wave pumps energy into its second harmonic, which in turn pumps energy into its subharmonic oblique wave.

The problem is formulated in Sec. II. The analysis for the combination-resonance case is contained in Sec. III, while the results for the second-harmonic case are stated in Sec. IV. The numerical procedure is discussed in Sec. V, while the numerical results are presented in Sec. VI.

II. PROBLEM FORMULATION

We consider nonlinear interactions of wave packets in a two-dimensional steady incompressible boundary layer. The equations describing the motion of the fluid are

$$\frac{\partial \tilde{u}}{\partial x} + \frac{\partial \tilde{v}}{\partial y} = 0 , \tag{1}$$

$$\frac{\partial \tilde{u}}{\partial t} + \tilde{u}\frac{\partial \tilde{u}}{\partial x} + \tilde{v}\frac{\partial \tilde{u}}{\partial y} = -\frac{\partial \tilde{p}}{\partial x} + \frac{1}{R}\nabla^2 \tilde{u} , \tag{2}$$

$$\frac{\partial \tilde{v}}{\partial t} + \tilde{u}\frac{\partial \tilde{v}}{\partial x} + \tilde{v}\frac{\partial \tilde{v}}{\partial y} = -\frac{\partial \tilde{p}}{\partial y} + \frac{1}{R}\nabla^2 \tilde{v} , \tag{3}$$

$$\tilde{u} = \tilde{v} = 0 \text{ at } y = 0 , \tag{4}$$

$$\tilde{u} \to 1 \text{ as } y \to \infty , \tag{5}$$

where

$$\nabla^2 = \frac{\partial^2}{\partial x^2} + \frac{\partial^2}{\partial y^2} .$$

Here, x and y are made dimensionless by using a reference length δ_r, the time is made dimensionless by using δ_r/U_∞, and the velocities are made dimensionless by using the free-stream velocity U_∞. The Reynolds number $R = U_\infty \delta_r/\nu$ with ν being the fluid kinematic viscosity.

The analysis is restricted to basic flows that are slightly nonparallel (i.e., vary slowly in the streamwise direction) and to disturbances that are small but finite. The slow variation is expressed by using the slow scale $x_1 = \epsilon_1 x$, where ϵ_1 is a small dimensionless quantity that characterizes the nonparallelism of the flow and can be related to R by $\epsilon_1 = R^{-1}$. The smallness of the amplitude of the disturbance is expressed by introducing the small dimensionless parameter ϵ. For a general solution, we assume that $\epsilon = O(\epsilon_1)$ so that the resulting expansion accounts simultaneously for the effects of nonparallelism and nonlinearity. When $\epsilon \ll \epsilon_1$, the nonlinear effects are negligible and the solution reduces to those obtained in Refs. 15 and 16. When $\epsilon \gg \epsilon_1$, the nonparallel effects are negligible and the solution reduces to equations with constant coefficients.

We assume that each flow quantity is the sum of a mean-flow quantity and an unsteady disturbance quantity, which is assumed to be much smaller than the mean-flow quantity. We can then express the velocity components and the pressure as

$$\tilde{u}(x,y,t) = U_0(x_1,y) + \epsilon u(x,y,t) , \tag{6}$$

$$\tilde{v}(x,y,t) = \epsilon_1 V_0(x_1,y) + \epsilon v(x,y,t) , \tag{7}$$

$$\tilde{p}(x,y,t) = P(x_1) + \epsilon p(x,y,t) , \tag{8}$$

where U_0, V_0, and P_0 are the nonparallel basic-flow quantities. Substituting Eqs. (6)–(8) into Eqs. (1)–(5) and subtracting the basic-flow quantities, we obtain

$$\frac{\partial u}{\partial x} + \frac{\partial v}{\partial y} = 0 , \tag{9}$$

$$\frac{\partial u}{\partial t} + U_0\frac{\partial u}{\partial x} + v\frac{\partial U_0}{\partial y} + \frac{\partial p}{\partial x} - \frac{1}{R}\nabla^2 u = -\epsilon_1 u\frac{\partial U_0}{\partial x_1} - \epsilon_1 V_0\frac{\partial u}{\partial y} - \epsilon u\frac{\partial u}{\partial x} - \epsilon v\frac{\partial u}{\partial y} , \tag{10}$$

$$\frac{\partial v}{\partial t} + U_0\frac{\partial v}{\partial x} + \frac{\partial p}{\partial y} - \frac{1}{R}\nabla^2 v = -\epsilon_1^2 u\frac{\partial V_0}{\partial x_1} - \epsilon_1 V_0\frac{\partial v}{\partial y} - \epsilon_1 v\frac{\partial V_0}{\partial y} - \epsilon u\frac{\partial v}{\partial x} - \epsilon v\frac{\partial v}{\partial y} , \tag{11}$$

$$u = v = 0 \text{ at } y = 0 , \tag{12}$$

$$u,\ v \to 0 \text{ as } y \to \infty . \tag{13}$$

Without loss of generality, we let $\epsilon = \epsilon_1$. To determine the wave-packet solutions of Eqs. (9)–(13), we use the method of multiple scales[17] and seek an expansion in the form

$$u = u_0(x_0,x_1,y,T_0,T_1) + \epsilon u_1(x_0,x_1,y,T_0,T_1) + \cdots , \tag{14}$$

$$v = v_0(x_0,x_1,y,T_0,T_1) + \epsilon v_1(x_0,x_1,y,T_0,T_1) + \cdots , \tag{15}$$

$$p = p_0(x_0,x_1,y,T_0,T_1) + \epsilon p_1(x_0,x_1,y,T_0,T_1) + \cdots , \tag{16}$$

where $x_0 = x$, $T_0 = t$, and $T_1 = \epsilon t$. Substituting Eqs. (14)-(16) into Eqs. (9)–(13) and equating coefficients of like powers of ϵ, we obtain

Order ϵ^0:

$$\frac{\partial u_0}{\partial x_0} + \frac{\partial v_0}{\partial y} = 0 , \tag{17}$$

$$\mathcal{L}_1(u_0, v_0, p_0) \equiv \frac{\partial u_0}{\partial T_0} + U_0\frac{\partial u_0}{\partial x_0} + v_0\frac{\partial U_0}{\partial y} + \frac{\partial p_0}{\partial x_0} - \frac{1}{R}\nabla_0^2 u_0 = 0 , \tag{18}$$

$$\mathfrak{L}_2(u_0, v_0, p_0) \equiv \frac{\partial v_0}{\partial T_0} + U_0 \frac{\partial v_0}{\partial x_0} + \frac{\partial p_0}{\partial y} - \frac{1}{R}\nabla_0^2 v_0 = 0\,, \quad (19)$$

$$u_0 = v_0 = 0 \text{ at } y = 0\,, \quad (20)$$

$$u_0, v_0 \to 0 \text{ as } y \to \infty\,, \quad (21)$$

Order ϵ:

$$\frac{\partial u_1}{\partial x_0} + \frac{\partial v_1}{\partial y} = -\frac{\partial u_0}{\partial x_1}\,, \quad (22)$$

$$\mathfrak{L}_1(u_1, v_1, p_1) = -\frac{\partial u_0}{\partial T_1} - U_0\frac{\partial u_0}{\partial x_1} - \frac{\partial p_0}{\partial x_1} + \frac{2}{R}\frac{\partial^2 u_0}{\partial x_0 \partial x_1} - u_0\frac{\partial U_0}{\partial x_1} - V_0\frac{\partial u_0}{\partial y} - u_0\frac{\partial u_0}{\partial x_0} - v_0\frac{\partial u_0}{\partial y}\,, \quad (23)$$

$$\mathfrak{L}_2(u_1, v_1, p_1) = -\frac{\partial v_0}{\partial T_1} - U_0\frac{\partial v_0}{\partial x_1} + \frac{2}{R}\frac{\partial^2 v_0}{\partial x_0 \partial x_1} - V_0\frac{\partial v_0}{\partial x_0} - v_0\frac{\partial V_0}{\partial y} - u_0\frac{\partial v_0}{\partial x_0} - v_0\frac{\partial v_0}{\partial y}\,, \quad (24)$$

$$u_1 = v_1 = 0 \text{ at } y = 0\,, \quad (25)$$

$$u_1,\ v_1 \to 0 \text{ as } y \to \infty\,, \quad (26)$$

where

$$\nabla_0^2 = \frac{\partial^2}{\partial x_0^2} + \frac{\partial^2}{\partial y^2}\,.$$

In what follows, we describe the details of the analysis for the combination-resonance case and only state the results for the second-harmonic resonance case.

III. COMBINATION RESONANCES

A. First-order problem

For the case of combination resonances, we consider three wave packets centered at the frequencies ω_1, ω_2, and ω_3. Then, we examine the resonances that might exist among them. Thus, the solution of Eqs. (17)–(21) is expressed as a linear combination of three Tollmien–Schlichting waves; that is,

$$u_0 = A_1(x_1, T_1)\zeta_{11}(y; x_1)\exp(i\theta_1) + A_2(x_1, T_1) \times \zeta_{12}(y; x_1)\exp(i\theta_2) + A_3(x_1, T_1)\zeta_{13}(y; x_1) \times \exp(i\theta_3) + \text{c.c.}, \quad (27)$$

$$v_0 = A_1(x_1, T_1)\zeta_{21}(y; x_1)\exp(i\theta_1) + A_2(x_1, T_1) \times \zeta_{22}(y; x_1)\exp(i\theta_2) + A_3(x_1, T_1)\zeta_{23}(y; x_1) \times \exp(i\theta_3) + \text{c.c.}, \quad (28)$$

$$p_0 = A_1(x_1, T_1)\zeta_{31}(y; x_1)\exp(i\theta_1) + A_2(x_1, T_1) \times \zeta_{32}(y; x_1)\exp(i\theta_2) + A_3(x_1, T_1)\zeta_{33}(y; x_1) \times \exp(i\theta_3) + \text{c.c.}, \quad (29)$$

where

$$\frac{\partial \theta_n}{\partial x_0} = k_n(x_1)\,, \quad \frac{\partial \theta_n}{\partial T_0} = -\omega_n \quad (n = 1, 2, 3)\,, \quad (30)$$

with the ω_n being real constants. The quasi-parallel Orr–Sommerfeld problems for these waves are

$$M_1(\zeta_{1n}, \zeta_{2n}; k_n) \equiv D\zeta_{2n} + ik_1\zeta_{1n} = 0\,, \quad (31)$$

$$M_2(\zeta_{1n}, \zeta_{2n}, \zeta_{3n}; k_n, \omega_n) \equiv i(U_0 k_n - \omega_n)\zeta_{1n} + \zeta_{2n} DU_0 + ik_1\zeta_{3n} - (1/R)(D^2 - k_n^2)\zeta_{1n} = 0\,, \quad (32)$$

$$M_3(\zeta_{1n}, \zeta_{2n}, \zeta_{3n}; k_n, \omega_n) \equiv i(U_0 k_n - \omega_n)\zeta_{2n} + D\zeta_{3n} - (1/R)(D^2 - k_n^2)\zeta_{2n} = 0\,, \quad (33)$$

$$\zeta_{1n} = \zeta_{2n} = 0 \text{ at } y = 0\,, \quad (34)$$

$$\zeta_{1n}, \zeta_{2n}, \to 0 \text{ as } y \to \infty\,, \quad (35)$$

where $D = \partial/\partial y$.

B. Second-order problem

Substituting Eqs. (27)–(29) into Eqs. (22)–(26), we find that the inhomogeneous parts in Eqs. (22)–(26) contain terms proportional to

$$\exp(i\theta_1)\,, \quad \exp(i\theta_2)\,, \quad \exp(i\theta_3)\,,$$
$$\exp[i(\theta_2 - \bar{\theta}_1)]\,, \quad \exp[i(\theta_1 + \theta_3)]\,, \quad \exp[i(\theta_2 - \bar{\theta}_3)]\,,$$

where the overbar indicates the complex conjugate. The terms that are proportional to these exponential expressions will create secular terms in the particular solutions for u_1, v_1, and p_1 if $k_3 \approx k_2 - k_1$ and $\omega_3 \approx \omega_2 - \omega_1$; that is, when a combination resonance exists among the waves. To quantitively express the nearness of the resonances, we introduce the two detuning parameters σ_1 and σ_2 defined by

$$\omega_3 - \omega_2 + \omega_1 = \epsilon\sigma_1\,, \quad (36)$$

$$\text{Real}(k_3 - k_2 + k_1) = \epsilon\sigma_2\,, \quad (37)$$

where $\sigma_n = O(1)$. The detuning σ_2 is based on the real parts of the interacting wavenumbers because the imaginary parts will disappear from the exponents in the interaction equations if the actual amplitudes of the waves are used, see Eqs. (57)–(59). Using Eq. (30), we have

$$\theta_1 + \theta_3 - \theta_2 = \int (k_1 + k_3 - k_2)dx_0 - (\omega_1 + \omega_3 - \omega_2)T_0$$
$$= \int (k_{1r} + k_{3r} - k_{2r})dx_0 + i\int (k_{1i} + k_{3i} - k_{2i})dx_0 - (\omega_1 + \omega_3 - \omega_2)T_0\,,$$

which upon using Eqs. (36) and (37) becomes

$$\theta_1 + \theta_3 - \theta_2 = \int \epsilon\sigma_2 dx_0 - \epsilon\sigma_1 T_0 + i\int (k_{1i} + k_{3i} - k_{2i})dx_0$$
$$= \int \sigma_2 dx_1 - \sigma_1 T_1 + i\int (k_{1i} + k_{3i} - k_{2i})dx_0\,.$$

Hence,

$$\theta_1 + \theta_3 = \int (k_1 + k_3)\,dx_0 - (\omega_1 + \omega_3)T_0 = \theta_2 + \phi + i\int (k_{1i} + k_{3i} - k_{2i})dx_0\,, \quad (38)$$

where k_{ni} stands for the imaginary part of k_n and

$$\phi = \int \sigma_2 dx_1 - \sigma_1 T_1\,. \quad (39)$$

Similarly, it follows from Eqs. (30), (36), and (37) that

$$\theta_2 - \bar{\theta}_3 = \theta_1 - \phi + i\int (k_{2i} + k_{3i} - k_{1i})dx_0\,, \tag{40}$$

$$\theta_2 - \bar{\theta}_1 = \theta_3 - \phi + i\int (k_{1i} + k_{2i} - k_{3i})dx_0\,. \tag{41}$$

To determine the A_n, we seek a particular solution for the second-order problem in the form

$$u_1 = \psi_{11}(y;x_1)\exp(i\theta_1) + \psi_{12}(y;x_1)\exp(i\theta_2) + \psi_{13}(y;x_1)\exp(i\theta_3) + \text{c.c.}, \tag{42}$$

$$v_1 = \psi_{21}(y;x_1)\exp(i\theta_1) + \psi_{22}(y;x_1)\exp(i\theta_2) + \psi_{23}(y;x_1)\exp(i\theta_3) + \text{c.c.}, \tag{43}$$

$$p_1 = \psi_{31}(y;x_1)\exp(i\theta_1) + \psi_{32}(y;x_1)\exp(i\theta_2) + \psi_{33}(y;x_1)\exp(i\theta_3) + \text{c.c.} \tag{44}$$

Substituting Eqs. (27)–(30) and (38)–(44) into Eqs. (22)–(26) and equating the coefficients of $\exp(i\theta_1)$, $\exp(i\theta_2)$, and $\exp(i\theta_3)$ on both sides, we obtain the following equations:

$$M_1(\psi_{1j}, \psi_{2j}; k_j) = d_{1j}\,, \tag{45}$$

$$M_2(\psi_{1j}, \psi_{2j}, \psi_{3j}; k_j, \omega_j) = d_{2j}\,, \tag{46}$$

$$M_3(\psi_{1j}, \psi_{2j}, \psi_{3j}; k_j, \omega_j) = d_{3j}\,, \tag{47}$$

$$\psi_{1j} = \psi_{2j} = 0 \text{ at } y = 0\,, \tag{48}$$

$$\psi_{1j}, \psi_{2j} \to 0 \text{ as } y \to \infty \tag{49}$$

for $j = 1$, 2, and 3, where the d_{ij} are given in Appendix A.

C. Adjoint problem

Since the homogeneous parts of Eqs. (45)–(49) are the same as Eqs. (31)–(35) and since the latter have a nontrivial solution, the inhomogeneous equations (45)–(49) have a solution if, and only if, the inhomogeneous parts are orthogonal to every solution of the adjoint homogeneous problem; that is,

$$\int_0^\infty (d_{1j}\zeta_{1j}^* + d_{2j}\zeta_{2j}^* + d_{3j}\zeta_{3j}^*)dy = 0 \quad \text{for } j = 1,\ 2,\ \text{and } 3\,, \tag{50}$$

where the ζ^*'s are the solutions of

$$M_1^*(\zeta_{2j}^*, \zeta_{3j}^*; k_j) \equiv ik_j\zeta_{2j}^* - D\zeta_{3j}^* = 0\,, \tag{51}$$

$$M_2^*(\zeta_{1j}^*, \zeta_{2j}^*, \zeta_{3j}^*;\ k_j, \omega_j) \equiv i(U_0k_j - \omega_j)\zeta_{3j}^* + \zeta_{2j}^*DU_0 - D\zeta_{1j}^* - (1/R)(D^2 - k_j^2)\zeta_{3j}^* = 0\,, \tag{52}$$

$$M_3^*(\zeta_{1j}^*, \zeta_{2j}^*, \zeta_{3j}^*; k_j, \omega_j) \equiv i(U_0k_j - \omega_j)\zeta_{2j}^* + ik_j\zeta_{1j}^* - (1/R)(D^2 - k_j^2)\zeta_{2j}^* = 0\,, \tag{53}$$

$$\zeta_{2j}^* = \zeta_{3j}^* = 0 \text{ at } y = 0\,, \tag{54}$$

$$\zeta_{1j}^*, \zeta_{2j}^* \to 0 \text{ as } y \to \infty\,. \tag{55}$$

Substituting for the d_{ij} from Appendix A into Eq. (50) and defining

$$a_j = A_j \exp\left(\int_{\bar{x}}^x k_{ji}\, dx_0\right), \tag{56}$$

we obtain the following differential equations for the evolution of a_1, a_2, and a_3:

$$\frac{1}{\omega_1'}\frac{\partial a_1}{\partial t} + \frac{\partial a_1}{\partial x} = \left(\epsilon_1\frac{h_{11}}{f_1} - k_{1i}\right)a_1 + \epsilon\frac{h_{123}}{f_1}a_2\bar{a}_3\exp(-i\phi)\,, \tag{57}$$

$$\frac{1}{\omega_2'}\frac{\partial a_2}{\partial t} + \frac{\partial a_2}{\partial x} = \left(\epsilon_1\frac{h_{22}}{f_2} - k_{2i}\right)a_2 + \epsilon\frac{h_{213}}{f_2}a_1a_3\exp(i\phi)\,, \tag{58}$$

$$\frac{1}{\omega_3'}\frac{\partial a_3}{\partial t} + \frac{\partial a_3}{\partial x} = \left(\epsilon_1\frac{h_{33}}{f_3} - k_{3i}\right)a_3 + \epsilon\frac{h_{312}}{f_3}a_2\bar{a}_1\exp(-i\phi)\,, \tag{59}$$

where $\omega_n' = d\omega_n/dk_n$ is the group velocity and ϕ is defined in Eq. (39). As discussed earlier, the detuning arising from the imaginary parts of the interacting wavenumbers does not appear in the exponents in the interaction equations (57)–(59). This is the reason for our basing the detuning on the real parts of the wavenumbers of the interacting waves, which is contained in ϕ. For spatial modulation only, $\sigma_1 = 0$ and $\partial a_n/\partial t = 0$; all the calculations presented in this paper are for this case. We note that Eqs. (57)–(59) account for the combined effects of the nonparallelism (i.e., growth of the boundary layer) and the nonlinear interaction. If $\epsilon \ll \epsilon_1$, the nonlinear interactions can be neglected and the spatial variations in Eqs. (57)–(59) reduce to the nonparallel solutions of Refs. 15 and 16. When $\epsilon_1 \ll \epsilon$, the effects of the nonparallelism are negligible; that is, one can set $\epsilon_1 = 0$ and all the coefficients in Eqs. (57)–(59) can be treated as constants.

IV. HARMONIC RESONANCE

The interaction between a fundamental Tollmien–Schlichting wave and its second harmonic is analyzed using a procedure similar to that outlined in the previous section. In this case, instead of Eqs. (57)–(59) we obtain

$$\frac{1}{\omega_1'}\frac{\partial a_1}{\partial t} + \frac{\partial a_1}{\partial x} = \left(\epsilon_1\frac{h_{11}}{f_1} - k_{1i}\right)a_1 + \epsilon\frac{h_{12}}{f_1}a_2\bar{a}_1\exp(i\phi)\,, \tag{60}$$

$$\frac{1}{\omega_2'}\frac{\partial a_2}{\partial t} + \frac{\partial a_2}{\partial x} = \left(\epsilon_1\frac{h_{22}}{f_2} - k_{2i}\right)a_2 + \epsilon\frac{h_{21}}{f_2}a_1^2\exp(-i\phi)\,, \tag{61}$$

where ϕ is defined in Eq. (41),

$$\epsilon\sigma_2 = \text{Real}(k_2 - 2k_1)\,, \quad \epsilon\sigma_1 = \omega_2 - 2\omega_1\,, \tag{62}$$

and f_1, f_2, h_{11}, h_{22}, h_{12}, and h_{21} are given in Appendices B and C.

For spatial modulation only, $\sigma_1 = 0$ and $\partial a_n/\partial t = 0$. All the calculations presented in this paper are for this case.

V. COMPUTATION PROCEDURE

A. Solution of first- and second-order problems

The same procedure is followed in solving the first- and second-order problems for both harmonic and combination resonances. Therefore, only the computation methodology for the solution of the first-order problem for the first mode is outlined here.

Equations (31)–(33) are expressed as a system of first-order differential equations in the form

$$\frac{dz}{dx} = Gz\,, \tag{63a}$$

where z is a 4×1 matrix with the elements

$$z_1=\zeta_{11}(y;x_1)\,,\quad z_2=D\zeta_{11}(y;x_1)\,,$$
$$z_3=\zeta_{21}(y;x_1)\,,\quad z_4=\zeta_{31}(y;x_1)\,, \tag{63b}$$

and G is a 4×4 matrix; its elements are given in Appendix D.

We start the integration of Eqs. (63) at $y=y_e$, where y_e is larger than the boundary-layer thickness. Hence, $U_0=1$, $DU_0=0$, and $D^2U_0=0$ at y_e. Then, the matrix G has constant coefficients at $y=y_e$ and Eqs. (63) have solutions of the form

$$z_i=\sum_{j=1}^{4} c_{ij}\exp(\lambda_j y)\quad \text{for } i=1,\ 2,\ 3, \text{ and } 4\,, \tag{64a}$$

where the c_{ij} are constants, the λ's are the solutions of

$$|G-\lambda I|=0\,, \tag{64b}$$

and I is the identity matrix. Equation (66) has the roots

$$\lambda_{1,2}=\pm k_1\,,\quad \lambda_{3,4}=\pm[k_1^2+i(k_1-\omega_1)R]^{1/2}\,. \tag{65}$$

Two of these roots have positive real parts that make the solution grow exponentially as $y\to\infty$; hence, they must be discarded to satisfy conditions (35). This leaves two linearly independent solutions that decay exponentially with y.

The eigenvalues are not known *a priori* and must be determined along with the eigenfunctions. For given values of ω_1 and R, we guess a value for k_1 and integrate Eqs. (63) from y_e to $y=0$. If the guessed value of k_1 does not satisfy the boundary conditions at $y=0$, k_1 is incremented using a Newton–Raphson scheme and the procedure is repeated until the boundary conditions are satisfied to within a specified accuracy. The integration is done by using a computer code developed by Scott and Watts.[18] This technique orthonormalizes the solution of the set of equations whenever a loss of independence is detected.

B. Solution of adjoint problem

The solution procedure is exactly the same as that for the first-order problem. The coefficients of the z matrix are

$$z_1=\zeta_{21}^*(y;x_1)\,,\quad z_2=D\zeta_{21}^*(y;x_1)\,,$$
$$z_3=\zeta_{31}^*(y;x_1)\,,\quad z_4=\zeta_{11}^*(y;x_1)\,, \tag{66}$$

and the adjoint problem has the same eigenvalues as the first-order problem.

C. Solvability conditions

The calculations are repeated at different streamwise locations to evaluate f_j, h_{jj}, k_j, and the other interaction integrals for a given frequency along the x axis. A fourth-order fixed step-size Runge–Kutta integration scheme is used to solve either Eqs. (57)–(59) for combination resonances or Eqs. (60) and (61) for harmonic resonances to find the amplitudes of the waves for different initial amplitudes of the respective modes.

VI. RESULTS AND DISCUSSION

The analysis presented in this paper is applicable to both two- and three-wave interactions. First, we present and discuss numerical results for the case of two-wave interactions. Then, we present and discuss numerical results for the interaction of three waves whose frequencies are such that $F_3=F_2-F_1$.

It follows from Eqs. (6), (27), (30), and (56) that, to a first approximation, the total streamwise velocity component is

$$\tilde{u}=U_0(y,x)+\epsilon\sum_{n=1}^{3}A_n(x)\zeta_{1n}(y,x)\exp\left(-\int k_{ni}\,dx\right)\times\exp\left(i\int k_{nr}\,dx-i\omega_n t\right)+O(\epsilon^2)\,,$$

or

$$\tilde{u}=U_0(y,x)+\sum_{n=1}^{3}a_n^*(x)\zeta_{1n}(y,x)\times\exp\left(i\int k_{nr}\,dx-i\omega_n t\right)+O(a_n^{*2})\,, \tag{67}$$

where

$$a_n^*=\epsilon a_n\,.$$

All results presented here are for the a_n^*, which we refer to as the "amplitudes" of the waves. In the absence of the interaction, Eqs. (57)–(59) become uncoupled and for the case of spatial modulation yield

$$a_n^*=a_n^*(0)\exp\left[\int\left(\frac{\epsilon_1 h_{11}}{f_1}-k_{1i}\right)dx\right]\,, \tag{68}$$

where $a_n^*(0)$ is the value of a_n^* at the reference location. We shall refer to the a_n^* in Eq. (68) as the noninteraction or linear values.

A. Two-wave interactions

The numerical results presented in Ref. 5 show that the amplitude of a wave $a_2^*=\epsilon a_2$ must exceed a critical value before it can generate and amplify its subharmonic due to the spatial detuning. In fact, the detuning in a boundary layer on a flat plate is so large that the critical value is approximately 29% of the mean flow. We note that, before this critical amplitude is reached, many other instability mechanisms would have taken place. In fact, the boundary layer would have already transitioned to turbulence. The analysis in Ref. 5 is for the case when the subharmonic wave has an infinitesimal amplitude. When the amplitude $a_1^*=\epsilon a_1$ of the subharmonic wave is not infinitesimal, its influence on a_2^* should be taken into account. The equations governing this influence are Eqs. (60) and (61) whose general solution is not yet available. The previous results of the parametric instability model[5] show that a_1^* oscillates about its noninteraction value until a_2^* reaches the critical value. Figures 1 and 2, obtained by numerically solving Eqs. (60) and (61), agree with this conclusion. Initially, a_2^* increases while a_1^* oscillates around its noninteraction value.

At $R\approx 580$, Fig. 1 shows that a_1^* starts to deviate sharply from its noninteraction value, while it follows

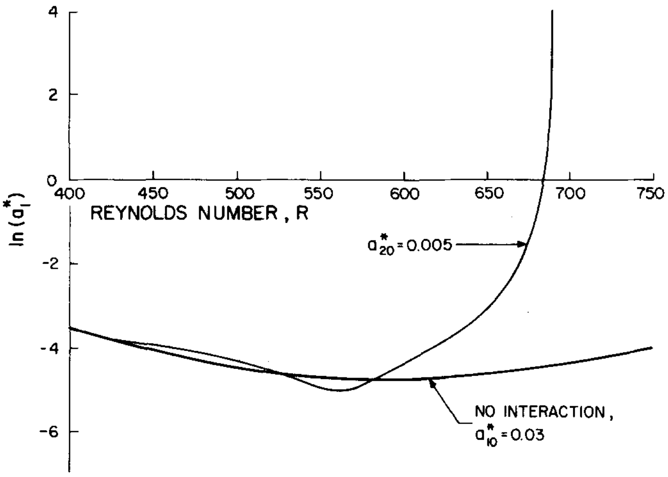

FIG. 1. Amplitude of a wave at $F_1=52\times10^{-6}$ involved in a subharmonic resonance with a fundamental wave at $F_2=104\times10^{-6}$.

from Fig. 2 that $\ln a_2^* \approx -1.25$ or $a_2^*=0.286$ at this location. Hence, when a_2^* is less than this critical value, the resonant interaction is unimportant and a_1^* can be approximated by its noninteraction (i.e., quasi-parallel linear) value; that is

$$a_1^* = a_{10}^* \exp\left(-\int k_{1i}\,dx + i\tau\right), \tag{69}$$

where a_{10}^* and τ are the initial amplitude and phase of the subharmonic wave, respectively. If we substitute Eq. (69) into Eq. (61) and neglect the nonparallel growth rate (i.e., $\epsilon_1 h_{22}/f_2$), we obtain

$$\frac{da_2^*}{dx} + k_{2i}a_2^* = \frac{h_{21}}{f_2} a_{10}^{*2} \exp\left(-\int (2k_{1i} + i\epsilon\sigma_2)dx + 2i\tau\right). \tag{70}$$

To determine an analytic approximation to the solution of Eq. (70), we consider the quasi-parallel case in which k_{ni}, h_{21}, f_2, and σ_2 are slowly varying functions of position. Thus, we let k_{ni}, h_{21}, f_2, and σ_2 assume their local values, but we neglect their derivatives. Then, the solution of Eq. (70) that satisfies the initial condition $a_2^* = a_2^*(0)$ at $x=0$ can be written as

$$a_2^* = \left(a_2^*(0) + \frac{h_{21}}{f_2(2k_{1i} + i\epsilon\sigma_2)} a_{10}^{*2} \exp(2i\tau)\right) \times \exp\left(-\int k_{2i}\,dx\right) - \frac{h_{21}}{f_2(2k_{1i}+i\epsilon\sigma_2)} a_{10}^{*2} \times \exp\left(-\int (2k_{1i} + i\epsilon\sigma_2\,dx + 2i\tau\right). \tag{71}$$

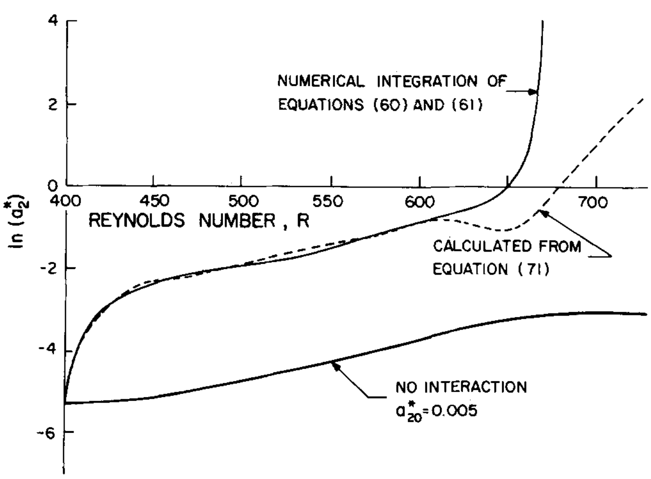

FIG. 2. Amplitude of the fundamental wave at $F_2=104\times10^{-6}$ involved in resonance with its subharmonic at $F_1=52\times10^{-6}$.

Equation (71) represents an approximation to a_2^* as long as it is less than the critical value needed to trigger the parametric instability in the subharmonic wave. We note that Eq. (71) contains the spatial detuning, which is very important in this problem. Had σ_2 and k_{1i} been small, Eqs. (69) and (71) would have been a poor approximation to the solutions of Eqs. (60) and (61) because of the importance of the resonant interaction. However, in a boundary layer, σ_2 is large so that the effect of resonant interactions is negligible.

Since the low frequency wave affects but is not affected by the high frequency wave when the amplitude of the high frequency wave is below 29% of the mean flow, we refer to the low frequency wave as the fundamental rather than the subharmonic wave and the high frequency wave as the second-harmonic rather than the fundamental wave. Next, we consider the generation and amplification of a second-harmonic wave by a fundamental Tollmien–Schlichting wave. We consider the following three cases: (i) fundamental wave is stable while its second harmonic is unstable, (ii) fundamental wave is unstable while its second harmonic is stable, and (iii) both fundamental and second-harmonic waves are unstable.

When the fundamental wave is initially stable while its second harmonic is unstable, a_1^* decays until it reaches the unstable region and then it increases as shown in Fig. 1. For Reynolds numbers less than 560, a_1^* oscillates around its noninteraction value, implying a small initial influence of its second harmonic on it. Thus, a_2^* can be approximated initially by Eq. (71). Figure 2 shows that the values obtained from Eq. (71), based on the quasi-parallel approximation, are in good agreement with those obtained by numerically integrating Eqs. (60) and (61) for $R \leqslant 560$. After a short initial distance, the second term on the right-hand side of Eq. (71) decays because the fundamental wave is stable (i.e., $k_{1i} > 0$). Then, a_2^* can be approximated by

$$a_2^* = \left(a_2^*(0) + \frac{h_{21}}{f_2(2k_{1i}+i\epsilon\sigma_2)} a_{10}^{*2}\exp(2i\tau)\right) \times \exp\left(-\int k_{2i}\,dx\right), \tag{72}$$

as long as a_2^* is less than the critical value. Thus, the effect of the fundamental wave on its second harmonic is to increase its initial amplitude and hence the effect is confined to the initial region. Figure 2 shows that the effect of the fundamental on the second harmonic is confined to the initial region near $R\approx 400$ when the amplitude of the second harmonic increases rapidly. Beyond $R \approx 425$, the amplitude of the fundamental wave has decayed so much that a_2^* assumes its normal linear

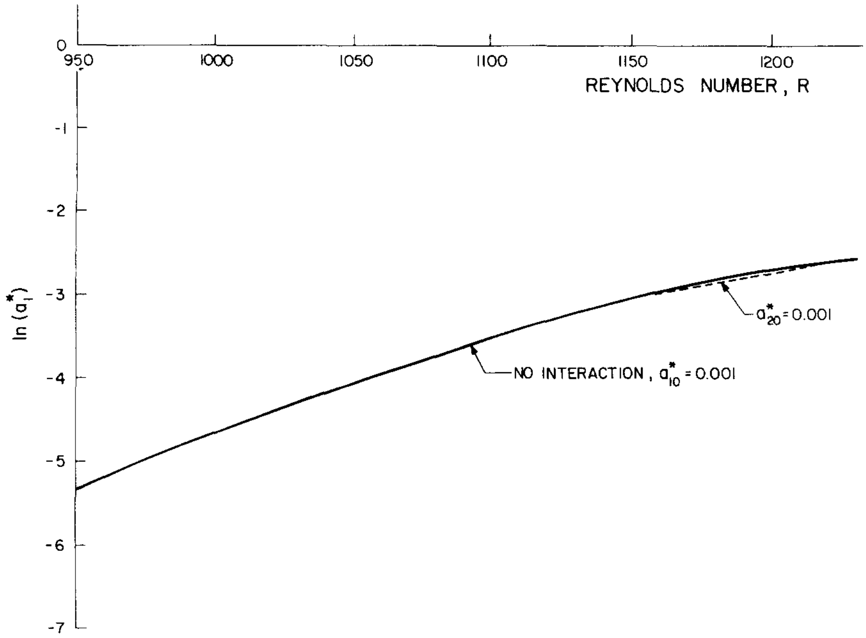

FIG. 3. Amplitude of a fundamental wave at $F_1 = 46.5\times10^{-6}$ involved in resonance with its harmonic at $F_2 = 93\times10^{-6}$.

growth rate until it reaches the region of strong interaction with a_1^* (i.e., subharmonic instability).

For the case when the fundamental wave is initially unstable while its second harmonic is stable, we performed calculations for waves with the frequencies $F_1 = 46.5\times10^{-6}$ and $F_2 = 93\times10^{-6}$. The fundamental wave is in the unstable region at $R = 950$ where the calculations are started. Thus, it is unstable downstream of $R = 950$. Figure 3, obtained by numerically integrating Eqs. (60) and (61), shows that a_1^* hardly deviates from its noninteraction (quasi-parallel linear) value. On the other hand, a_2^* increases many orders of magnitude above its noninteraction values, even for small initial amplitudes of the fundamental wave as shown in Fig. 4. In these calculations, the initial amplitude of the second-harmonic wave is taken to be 0.1% while the initial amplitudes of the fundamental wave are 0.1% and 0.5%. Since a_1^* hardly deviates from its noninteraction value, the quasi-parallel solution is expected to be a good approximation to a_2^*. Figure 4 shows that the values obtained from Eq. (71) oscillate about those obtained by numerically integrating Eqs. (60) and (61). Since the initial values are very small, a_2^* does not reach the critical value to influence a_1^*. After a short initial distance, the first term on the right-hand side of Eq. (71) decays and a_2^* can be approximated by

$$a_2^* = -\frac{h_{21}}{f_2(2k_{1i} + i\epsilon\sigma_2)}\, a_{10}^{*2} \exp\left[-\left(\int 2k_{1i} + i\epsilon\sigma_2\right)dx + 2i\tau\right], \tag{73}$$

as long as a_2^* is less than the critical value. Equation (73) shows that the effect of the interaction is to produce

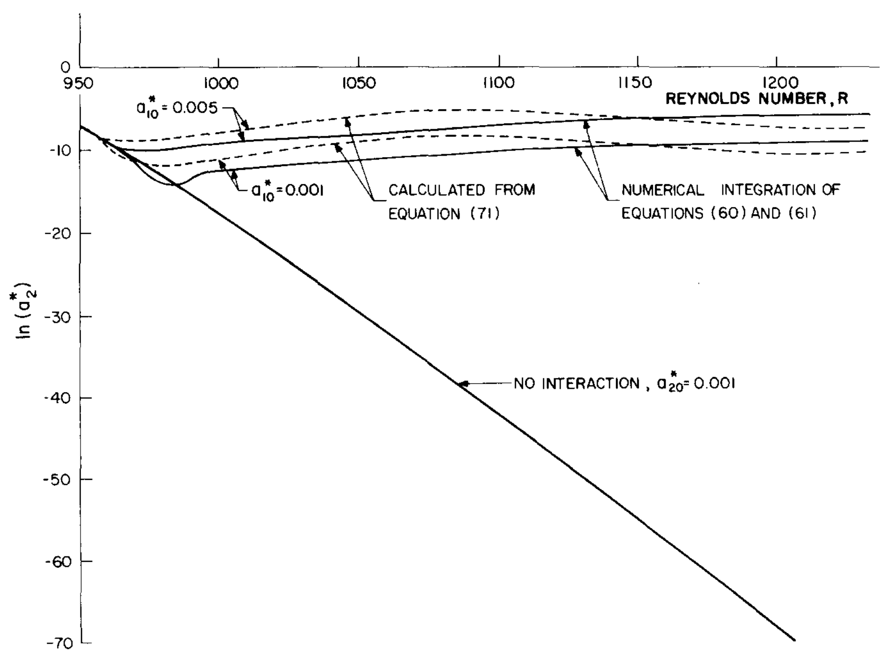

FIG. 4. Amplitude of the second-harmonic wave at $F_2 = 93\times10^{-6}$ when it is involved in resonance with a wave at $F_1 = 46.5\times10^{-6}$.

a second-harmonic wave that grows approximately at a rate that is twice that of the fundamental wave, in agreement with recent experiments conducted by Saric and Reynolds.[9]

For the case when both waves are unstable, we performed numerical calculations for waves having the frequencies $F_1 = 52 \times 10^{-6}$ and $F_2 = 104 \times 10^{-6}$ starting near $R \approx 600$. Figure 5 shows that initially a_1^* deviates slightly from its noninteraction (quasi-parallel linear) values. Hence, the quasi-parallel solution is initially expected to be a good approximation to a_2^*. Figure 6 shows that the numerical values obtained from Eq. (71) are in good agreement with those obtained by numerically integrating Eqs. (60) and (61) when a_2^* is less than 0.29, owing to the insignificance of the resonance. Thus, in this case, the effect of the interaction on the second-harmonic wave is to increase its initial amplitude and to produce a term that grows at a rate that is twice the growth rate of the fundamental wave. Due to the fact that both waves are initially unstable, the interaction is more effective in this case than in the preceding two cases.

B. Three-wave interactions

In their experimental studies, Kachanov *et al.*,[8] Saric and Reynolds,[9] Miksad,[7] Norman,[10] and Sato[6] introduced two separate waves of different frequencies into the flow that was being studied. They observed the growth of a wave whose frequency is equal to the difference frequency. Kachanov *et al.* used the frequency pairs $F_1 = 88 \times 10^{-6}$ and $F_2 = 104 \times 10^{-6}$ and $F_1 = 88 \times 10^{-6}$ and $F_2 = 120 \times 10^{-6}$ to analyze the growth of the associated difference-harmonic waves at $F_3 = 16 \times 10^{-6}$ (i.e., $F_3 = F_2 - F_1$) and $F_3 = 32 \times 10^{-6}$ in a boundary-layer flow over a flat plate. Unfortunately, they did not present data showing the variation of the amplitude of the difference frequency with distance. Consequently, we were unable to compare quantitatively our results with their experiment, and we had to settle for a qualitative comparison. Using the same frequency pairs, we determined the amplitudes of the fundamental waves (a_1^* and a_2^*) and the difference-harmonic wave a_3^* by numerically solving Eqs. (57)–(59). Figures 7 and 8 show the large increases in the amplitudes of the difference-harmonic waves due to the nonlinear interaction of the waves with the frequencies F_1 and F_2. The amplitude of the difference-harmonic wave at $R \approx 715$ is increased by 120–200 times its noninteraction value.

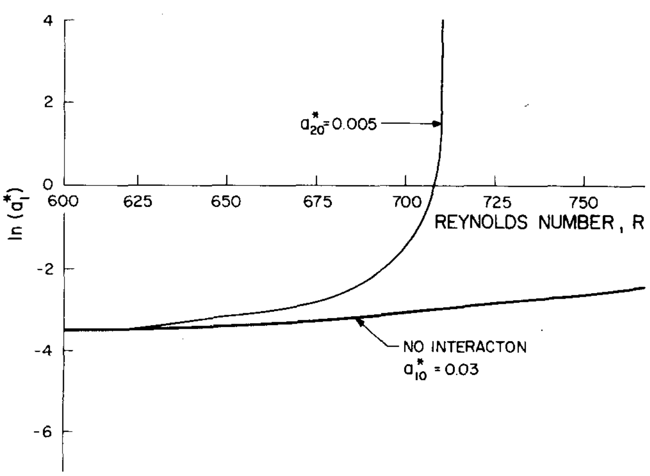

FIG. 5. Amplitude of fundamental wave at $F_1 = 52 \times 10^{-6}$ involved in resonance with its harmonic at $F_2 = 104 \times 10^{-6}$.

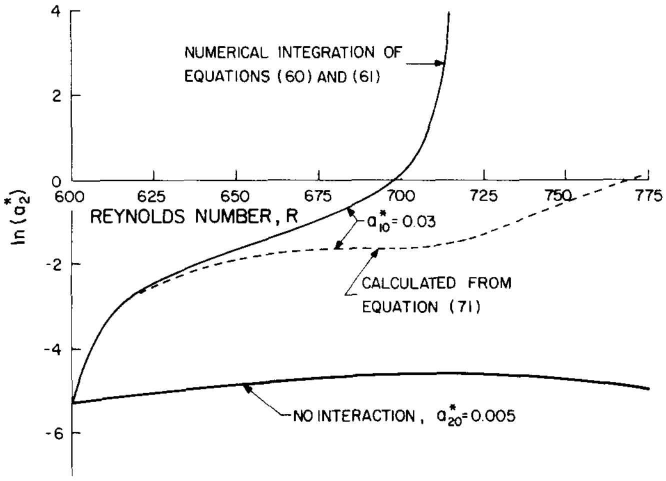

FIG. 6. Amplitude of the second-harmonic wave at $F_2 = 104 \times 10^{-6}$ when it is involved in resonance with a wave at $F_1 = 52 \times 10^{-6}$.

However, the amplitudes of the fundamental waves change very little from their noninteraction values as shown in Fig. 9 for $F_1 = 88 \times 10^{-6}$, owing to the large spatial detuning that wipes out the effect of resonance unless the initial amplitudes are very large. Thus, a_1^* and a_2^* can be approximated by their quasi-parallel linear values; that is,

$$a_1^* = a_{10}^* \exp\left(-\int k_{1i} dx + i\tau_1\right),$$
$$a_2^* = a_{20}^* \exp\left(-\int k_{2i} dx + i\tau_2\right), \tag{74}$$

where a_{10}^* and a_{20}^* are the initial amplitudes and τ_1 and τ_2 are the initial phases of the fundamental waves. Substituting Eq. (74) into Eq. (59) and neglecting the nonparallel effects, we obtain

$$\frac{da_3^*}{dx} + k_{3i} a_3^* = \frac{h_{312}}{f_3} a_{10}^* a_{20}^* \exp\left(-\int (k_{1i} + k_{2i} + i\epsilon\sigma_2) dx + i(\tau_1 + \tau_2)\right). \tag{75}$$

The solution of Eq. (75) that satisfies the initial condition $a_3^* = a_3^*(0)$ at $x = 0$ can be expressed as

$$a_3^* = \left(a_3^*(0) + \frac{h_{312}}{f_3(k_{1i} + k_{2i} + i\epsilon\sigma_2)} a_{10}^* a_{20}^* \exp(i\tau_1 + i\tau_2)\right) \times \exp\left(-\int k_{3i}\, dx\right) - \frac{h_{312}}{f_3(k_{1i} + k_{2i} + i\epsilon\sigma_2)} a_{10}^* a_{20}^* \times \exp\left(-\int (k_{1i} + k_{2i} + i\epsilon\sigma_2) dx + i(\tau_1 + \tau_2)\right). \tag{76}$$

Equation (76) represents an approximation to a_3^* as long as the amplitudes of the fundamental waves do not deviate from their noninteraction (quasi-parallel linear) values. Figures 7 and 8 show that Eq. (76) is initially

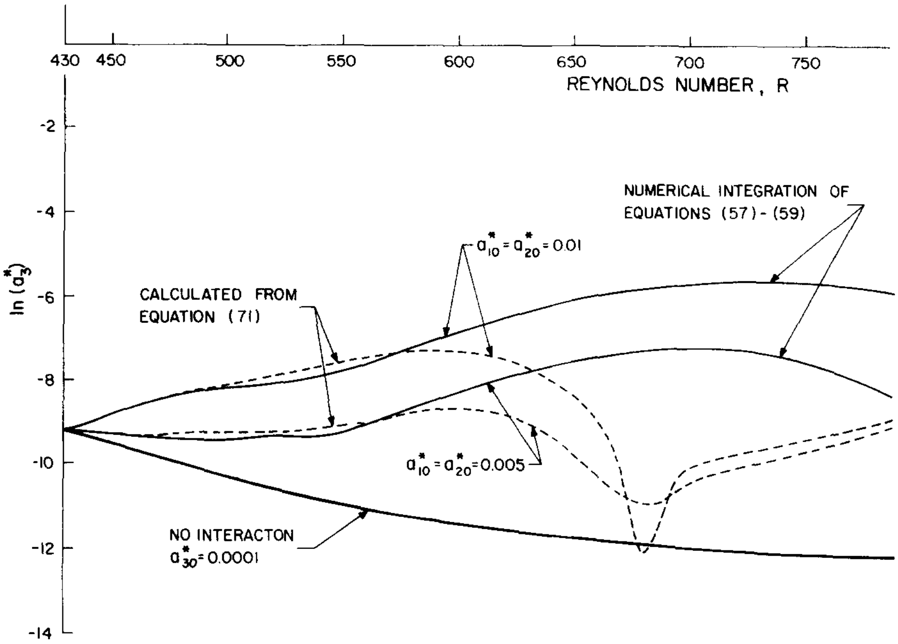

FIG. 7. Amplitude of the difference-harmonic wave at $F_3 = 32\times10^{-6}$ generated from a combination resonance of $F_1 = 88\times10^{-6}$ and 120×10^{-6}.

in good agreement with solutions obtained by numerically integrating Eqs. (57)–(59). Had $k_{1i} + k_{2i} + i\epsilon\sigma_2$ been small, Eqs. (74) and (76) would have been a poor approximation to the solutions of Eqs. (57)–(59) owing to the resonant interaction. However, in a boundary layer, σ_2 is large so that the effect of resonant interactions is negligible.

According to Eq. (76), the difference-harmonic wave grows at a rate that is the sum of the growth rates of the fundamental waves. Since the fundamental waves are unstable at $R = 430$, where the calculations are started, the difference-harmonic wave amplifies considerably, in spite of the fact that it is stable in the absence of the interaction. However, this instability is not of the explosive type due to the spatial detuning. These results are in qualitative agreement with the experimental observations of Refs. 6–10.

ACKNOWLEDGMENTS

The authors appreciate the comments of Dr. W. S. Saric very much.

This work was supported by the Fluid Dynamics Program of the United States Office of Naval Research under Contract No. N00014-75-C-0381 and the National Aeronautics and Space Administration, Langley Research Center under Grant No. NSG-1255.

APPENDIX A

$$d_{1j} = -\left(\frac{\partial A_j}{\partial x_1}\zeta_{1j} + A_j\frac{\partial \zeta_{1j}}{\partial x_1}\right), \tag{A1}$$

$$d_{2j} = d_{2j0} + d_{2j1}, \tag{A2}$$

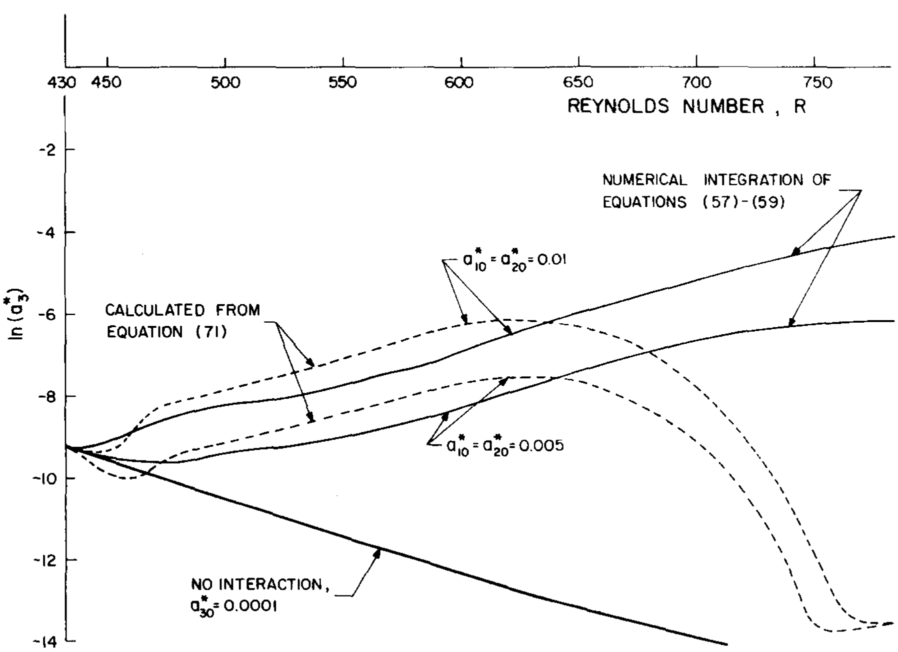

FIG. 8. Amplitude of the difference-harmonic wave at $F_3 = 16\times10^{-6}$ generated from a combination resonance of $F_1 = 88\times10^{-6}$ and $F_2 = 104\times10^{-6}$.

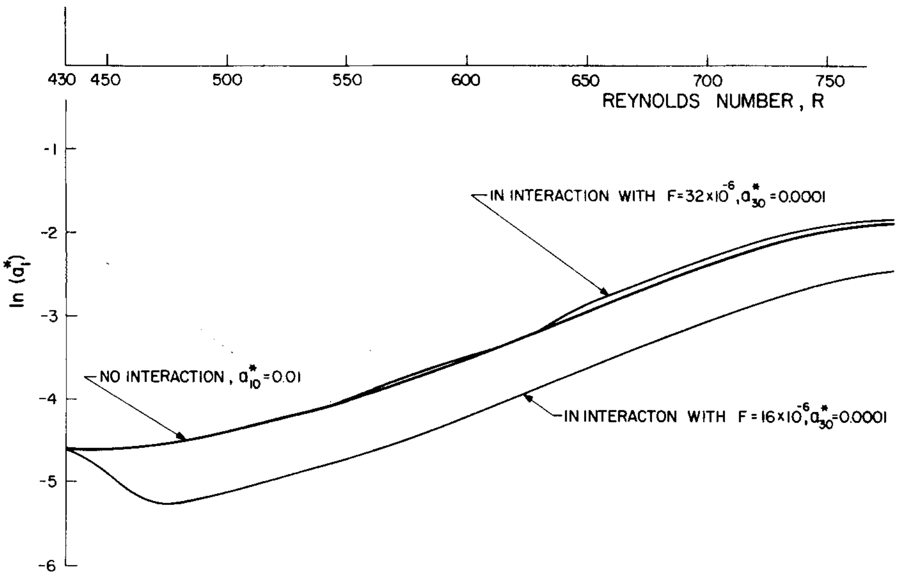

FIG. 9. Amplitude of the fundamental wave at $F_1=88\times10^{-6}$ involved in a combination resonance with two waves at $F_2=104\times10^{-6}$ and $F_3=16\times10^{-6}$.

$$d_{2j0}=-\frac{\partial A_j}{\partial T_1}\zeta_{1j}\left(U_0\zeta_{1j}+\zeta_{3j}-\frac{2i}{R}k_j\zeta_{1j}-V_0D\zeta_{1j}\right)\frac{\partial A_j}{\partial x_1}-\left[U_0\frac{\partial\zeta_{1j}}{\partial x_1}+V_0D\zeta_{1j}+\frac{\partial\zeta_{3j}}{\partial x_1}-\frac{2i}{R}\left(k_j\frac{\partial\zeta_{1j}}{\partial x_1}+\frac{dk_j}{dx_1}\zeta_{1j}\right)+\frac{\partial U_0}{\partial x_1}\zeta_{1j}\right]A_j\,, \tag{A3}$$

$$d_{211}=[i(k_2-\bar{k}_3)\zeta_{12}\bar{\zeta}_{13}+\zeta_{22}D\bar{\zeta}_{13}+D\zeta_{12}\zeta_{23}]A_2\bar{A}_3\times\exp[-i\phi-(k_{2i}+k_{3i}-k_{1i})dx_0]\,, \tag{A4}$$

$$d_{221}=[i(k_1+k_3)\zeta_{11}\zeta_{13}+\zeta_{21}D\zeta_{13}+D\zeta_{11}\zeta_{23}]A_1A_3\times\exp[i\phi-(k_{1i}+k_{3i}-k_{2i})dx_0]\,, \tag{A5}$$

$$d_{231}=(-i\bar{k}_1\bar{\zeta}_{11}\zeta_{12}+ik_2\zeta_{12}\bar{\zeta}_{11}+\zeta_{22}D\bar{\zeta}_{11}+D\zeta_{12}\bar{\zeta}_{21})A_2\bar{A}_1\times\exp[-i\phi-(k_{1i}+k_{2i}-k_{3i})dx_0]\,, \tag{A6}$$

$$d_{3j}=d_{3j0}+d_{3j1}\,, \tag{A7}$$

$$d_{3j0}=\frac{\partial A_j}{\partial T_1}\zeta_{2j}-\left(U_0\zeta_{2j}-\frac{2i}{R}k_j\zeta_{2j}\right)\frac{\partial A_j}{\partial x_1}-\left[U_0\frac{\partial\zeta_{2j}}{\partial x_1}+V_0D\bar{\zeta}_{2j}+\zeta_{2j}DV_0-\frac{2i}{R}\left(\frac{dk_j}{dx_1}\zeta_{2j}+k_j\frac{\partial\zeta_{2j}}{\partial x_1}\right)\right]A_j\,, \tag{A8}$$

$$d_{311}=(-i\bar{k}_3\zeta_{12}\bar{\zeta}_{23}+ik_2\zeta_{22}\bar{\zeta}_{13}+\zeta_{22}D\bar{\zeta}_{23}+D\zeta_{22}\bar{\zeta}_{23})A_2\bar{A}_3\times\exp[-i\phi-(k_{2i}+k_{3i}-k_{1i})dx_0]\,, \tag{A9}$$

$$d_{321}=(ik_3\zeta_{11}\zeta_{23}+ik_1\zeta_{21}\zeta_{13}+\zeta_{21}D\zeta_{23}+D\zeta_{21}\zeta_{23})A_1A_3\times\exp[-i\phi-(k_{1i}+k_{3i}-k_{2i})dx_0]\,, \tag{A10}$$

$$d_{331}=(-i\bar{k}_1\bar{\zeta}_{21}+ik_2\zeta_{22}\bar{\zeta}_{11}+\zeta_{22}D\bar{\zeta}_{21}+D\zeta_{22}\bar{\zeta}_{21})A_2\bar{A}_1\times\exp[-i\phi-(k_{1i}+k_{2i}-k_{3i})dx_0]\,. \tag{A11}$$

APPENDIX B

$$f_j=\int_0^\infty\left\{-\zeta_{1j}\zeta_{1j}^*-\left[\left(U_0-\frac{2ik_j}{R}\right)\zeta_{1j}+\zeta_{3j}\right]\zeta_{2j}^*-\left(U_0-\frac{2ik_j}{R}\right)\zeta_{2j}\zeta_{3j}^*\right\}dy\quad(j=1,2,3)\,, \tag{B1}$$

$$h_{jj}=\int_0^\infty\left\{\frac{\partial\zeta_{1j}}{\partial x_1}\zeta_{1j}^*+\left[U_0\frac{\partial\zeta_{1j}}{\partial x_1}+\frac{\partial\zeta_{3j}}{\partial x_1}+V_0D\zeta_{1j}-\frac{2i}{R}\left(k_j\frac{\partial\zeta_{1j}}{\partial x_1}+\frac{dk_j}{dx_1}\zeta_{1j}\right)+\frac{\partial U_0}{\partial x_1}\zeta_{1j}\right]\zeta_{2j}^*+\left[\left(U_0-\frac{2ik_j}{R}\right)\frac{\partial\zeta_{2j}^*}{\partial x_1}+V_0D\zeta_{2j}+\zeta_{2j}DV_0-\frac{2i}{R}\frac{dk_j}{dx_1}\zeta_{2j}\right]\zeta_{3j}^*\right\}dy\quad(j=1,2,3)\,, \tag{B2}$$

$$h_{123}=\int_0^\infty\{[i(k_2-\bar{k}_3)\zeta_{12}\bar{\zeta}_{13}+\zeta_{22}D\bar{\zeta}_{13}+D\zeta_{12}\bar{\zeta}_{23}]\zeta_{21}^*+(-i\bar{k}_3\zeta_{12}\bar{\zeta}_{23}+ik_2\zeta_{22}\bar{\zeta}_{13}+\zeta_{22}D\bar{\zeta}_{23}+D\zeta_{22}\bar{\zeta}_{23})\zeta_{31}^*\}dy\,, \tag{B3}$$

$$h_{213}=\int_0^\infty\{[i(k_1+k_3)\zeta_{11}\zeta_{13}+\zeta_{21}D\zeta_{13}+D\zeta_{11}\zeta_{23}]\zeta_{22}^*+(ik_3\zeta_{11}\zeta_{23}+ik_1\zeta_{21}\zeta_{13}+\zeta_{21}D\zeta_{23}+D\zeta_{21}\zeta_{23})\zeta_{32}^*\}dy\,, \tag{B4}$$

$$h_{312}=\int_0^\infty\{[i(k_2-\bar{k}_1)\zeta_{12}\bar{\zeta}_{11}+\zeta_{22}D\bar{\zeta}_{11}+D\zeta_{12}\bar{\zeta}_{21}]\zeta_{23}^*+(-i\bar{k}_1\bar{\zeta}_{21}\zeta_{12}+ik_2\zeta_{22}\bar{\zeta}_{11}+\zeta_{22}D\bar{\zeta}_{21}+D\zeta_{22}\bar{\zeta}_{21})\zeta_{33}^*\}dy\,. \tag{B5}$$

APPENDIX C

$$h_{12}=\int_0^\infty\{[\zeta_{22}D\bar{\zeta}_{11}+\bar{\zeta}_{21}D\zeta_{12}+i(k_2-\bar{k}_1)\zeta_{12}\bar{\zeta}_{11}]\zeta_{21}^*+[ik_2\zeta_{22}\bar{\zeta}_{11}-i\bar{k}_1\bar{\zeta}_{21}\zeta_{12}+\zeta_{22}D\bar{\zeta}_{21}+\bar{\zeta}_{21}D\zeta_{22}]\zeta_{31}^*\}dy\,, \tag{C1}$$

$$h_{21}=\int_0^\infty\{[(ik_1\zeta_{11}^2+\zeta_{21}D\zeta_{11})\zeta_{22}^*+(ik_1\zeta_{11}\zeta_{21}+\zeta_{21}D\zeta_{21})\zeta_{32}^*]\}dy\,. \tag{C2}$$

APPENDIX D

$$g_{11}=0,\quad g_{12}=1,\quad g_{13}=0\,,\quad g_{14}=0\,, \tag{D1}$$

$$g_{21}=i(U_0k-\omega)R+k^2\,,\quad g_{22}=0,\quad g_{23}=R\frac{dU_0}{\nu}\,,\quad g_{24}=ikR\,, \tag{D2}$$

$$g_{31}=-ik, \quad g_{32}=g_{33}=g_{34}=0, \tag{D3}$$

$$g_{41}=0, \quad g_{42}=-ik/R, \quad g_{43}=-[i(U_0k-\omega)+k^2/R], \quad g_{44}=0; \tag{D4}$$

Q is a 2×4 matrix consisting of the last two rows of the matrix B^{-1}. The matrix B has the elements:

$$b_{11}=b_{12}=b_{13}=b_{14}=1, \tag{D5}$$

$$b_{21}=-k, \quad b_{22}=\tilde{k}, \quad b_{23}=k, \quad b_{24}=-\tilde{k}, \tag{D6}$$

$$b_{31}=i, \quad b_{32}=ik/\tilde{k}, \quad b_{33}=-i, \quad b_{34}=-ik/\tilde{k}, \tag{D7}$$

$$b_{41}=(\omega/k-1), \quad b_{42}=0, \quad b_{43}=(\omega/k-1), \quad b_{44}=0, \tag{D8}$$

where

$$\tilde{k}=[k^2+i(k-\omega)R]^{1/2}. \tag{D9}$$

[1]H. Sato, J. Phys. Soc. J. **14**, 1797 (1959).
[2]O. Wehrmann and R. Wille, in *Boundary Layer Research*, edited by H. Görtler (Springer-Verlag, Berlin, 1958), p. 387.
[3]I. S. Kachanov, V. V. Kozlov, and V. Levchenko, Fluid Dyn. 3, 4 (1977).
[4]R. E. Kelly, J. Fluid Mech. **27**, 657 (1967).
[5]A. H. Nayfeh and A. N. Bozatli, Phys. Fluids **22**, 805 (1979).
[6]H. Sato, J. Fluid Mech. **44**, 741 (1970).
[7]R. W. Miksad, J. Fluid Mech. **59**, 1 (1973).
[8]I. S. Kachanov, V. V. Kozlov, and V. Levchenko, presented at the AIAA 11th Fluid and Plasma Dynamics Conference, Seattle, Washington (1978), paper 78-1131.
[9]W. S. Saric and G. A. Reynolds, presented at the International Union of Theoretical and Applied Mechanics Symposium on Laminar-Turbulent Transition, Stuttgart, Federal Republic of Germany (1979).
[10]R. S. Norman, Ph.D. dissertation, Illinois Institute of Technology (1972).
[11]A. D. D. Craik, J. Fluid Mech. **50**, 393 (1971).
[12]A. D. D. Craik and J. A. Adam, Proc. R. Soc. London Ser. A **363**, 243 (1978).
[13]A. D. D. Craik, Proc. R. Soc. London Ser. A **363**, 257 (1978).
[14]A. H. Nayfeh and A. N. Bozatli, presented at the AIAA 12th Fluid and Plasma Dynamics Conference, Williamsburg, Virginia (1979), paper 79-1496.
[15]A. H. Nayfeh, W. S. Saric, and D. T. Mook, Arch. Mech. Stosow **26**, 401 (1974).
[16]W. S. Saric and A. H. Nayfeh, Phys. Fluids **18**, 945 (1975).
[17]A. H. Nayfeh, *Perturbation Methods* (Wiley, New York, 1973), Chap. 6.
[18]M. R. Scott and H. Watts, SIAM J. Numer. Anal. **14**, 40 (1977).